Low SNR Regime Capacity Analysis of MIMO Systems Using Directional Antennas

Pooya Shariatpanahi[1], Amir Ahmad Shishegar[1], Babak Hossein Khalaj[1],
Amir Hessam Salavati[1], Hamidreza Saligheh Rad[2]

1: Department of Electrical Engineering, Sharif University of Technology, Azadi Ave., Tehran, Iran.
2: School of Engineering and Applied Sciences, Harvard University, Cambridge, MA 02138, USA.
{email: pooya@ee.sharif.edu, shishegar@sharif.edu, khalaj@sharif.edu, salavati@ee.sharif.edu, hamid@seas.harvard.edu}

***Abstract*—In this paper, we evaluate the capacity of Multiple-Input Multiple-Output (MIMO) systems using directional antennas in non-isotropic scattering environments. Our analytical analysis approach results in closed-form approximate formulas in low Signal to Noise Ratio (SNR) regime (in contrast to previous research works which have investigated the same problem by employing experimental or simulation frameworks). We propose an upper bound for the introduced approximate error. Our results show that MIMO systems equipped with directional antennas may have much higher capacity in non-isotropic scattering environments compared to MIMO systems equipped with omni-directional antennas. We also evaluate our results by some numerical examples in communication systems employing Square Microstrip Patch multi-element antennas (MEA)s as well as Horn MEAs.**

Keywords: **MIMO Channel Capacity, Directional Antennas, Low SNR Performance.**

I. Introduction

Recently, there has been a great interest in employing multiple antennas at the transmitter and/or the receiver to enhance the system capacity, and it has been shown that this technique considerably enhances the system capacity [1]. Each antenna element in a MIMO wireless system has specific physical characteristics such as polarization and radiation pattern. It has been studied in the literature that these characteristics have great effects on the overall MIMO system performance [2], [3]. In [2], a capacity analysis is proposed based on indoor measurements which shows the effect of the antenna polarization on the system capacity. Also, in [3], with the help of experimental results, the effect of different possible pattern and polarization configurations on the system performance is studied. In a recent work in [4], the effect of antenna physics on the multielement system capacity has been investigated. In a simulation-based context, it has been shown in [4] that using directive antennas as elements of a MIMO system can enhance the system capacity. The channel model employed in [4] is an extension of the "one-ring" model to spherical scattering environments which has enabled the authors to analyze the system performance in 3D Rayleigh fading environments. Another example considering the same problem is [5] which has proposed a measurement-based framework to analyze the effect of directional antenna arrays on the performance of indoor and outdoor MIMO systems. Also, in [6] the authors use numerical examples to discuss the information capacity of directional antennas compared to omnidirectional antennas.

As indicated above, most of the previous research works on the capacity analysis of MIMO systems using directional antennas are based on measurements and/or simulations. In this paper, in contrast to previous research works, we develop an analytical framework to analyze the capacity enhancement of the MIMO systems using directional antennas. To achieve this objective, we consider a multipath fading channel model in which the Angle of Arrival (AoA) at an antenna element is characterized by a Probability Distribution Function (p.d.f.). Two broadly accepted candidates for AoA distribution are truncated Laplace and truncated Normal distributions [10]. Also, our analysis is performed in low SNR regime that enables us to use the well-known result indicating that the power gain provided by MIMO systems in low SNR regime is proportional to the number of received antennas compared to single antenna case [7]. We derive a closed-form approximate result for the capacity of MIMO systems using directional antennas supported with an upper bound on the approximation error. In addition, we numerically evaluate our results by some examples such as Square Microstrip Patch Antennas as well as Horn Antennas. The numerical illustrations verify the appropriateness of our approximation approach.

II. System Model

A. Review of the Model For the Narrowband Fading Channel

In a flat fading channel model, the expression for the received signal in a mulipath fading channel is as follows [8]:

$$r(t) = \{u(t)e^{j2\pi f_c t}(\sum_{n=1}^{N} \sqrt{2\pi G(\theta_n)}\alpha_n(t)e^{-j\phi_n(t)})\} \quad (1)$$

where $u(t)$ is the baseband representation of the transmitted signal, f_c is the carrier frequency, n represents the index of the path in a multipath set, ϕ_n is the phase shift of the corresponding path, N is the total number of paths, and $\sqrt{2\pi G(\theta_n)}$ represents the normalized antenna amplitude gain for the nth path such that $\int_0^{2\pi} G(\theta)d\theta = 1$. If we assume that the transmitted signal is an unmodulated carrier signal (i.e., $s(t) = \Re\{e^{j2\pi f_c t}\}$, where $\Re\{.\}$ denotes the real part

978-1-4244-2751-2/08/$25.00 ©2008 IEEE

operator.), then the received signal is as follows [8]:

$$r(t) = r_I(t)\cos(2\pi f_c t) + r_Q(t)\sin(2\pi f_c t) \quad (2)$$

where the in-phase and quadrature components are $r_I(t) = \sum_{n=1}^{N}\sqrt{2\pi G(\theta_n)}\alpha_n(t)\cos(\phi_n(t))$ and $r_Q(t) = \sum_{n=1}^{N}\sqrt{2\pi G(\theta_n)}\alpha_n(t)\sin(\phi_n(t))$. Thus, the mean power of the received signal, $E[r(t)^2]$, is as follows ($n \gg 1$):

$$\begin{aligned} E[r(t)^2] &= E[r_I(t)^2] = 0.5\sum_n 2\pi G(\theta_n)E[\alpha_n^2] \\ &= 2\pi\int_0^{2\pi} G(\theta)f_\Theta(\theta)d\theta \end{aligned} \quad (3)$$

where we have assumed the distribution of $f_\Theta(\theta)$ for AoA, and we have normalized the total receive power such that $E[r(t)^2] = 1$ when using omnidirectional antenna (i.e., $G(\theta) = 1/2\pi$).

B. MIMO Channel Capacity in Low SNR Regime

Consider a narrowband MIMO system with n_t transmit and n_r receive antennas, where the MIMO channel is characterized by an $n_r \times n_t$ element matrix H with additive white gaussian noise at each receiver antenna. It is known that the capacity of the MIMO channel when there is no Channel State Information (CSI) at the transmitter is [7]:

$$\begin{aligned} C &= \sum_{i=1}^{n_{min}} E[\log_2(1+\frac{\gamma_0}{n_t}\lambda_i^2)] \\ &\approx \frac{\gamma_0}{n_t}E[tr[HH^*]]\log_2 e \\ &= (n_r\gamma_0\log_2 e)E[h^2] \end{aligned} \quad (4)$$

where $n_{min} = \min(n_t, n_r)$, γ_0 is the transmitted signal to noise ratio (snr), λ_is are the singular values of the channel matrix, and we have assumed that channel statistics of all the antennas are identical. Also, note that $E[h^2] = E[r(t)^2]$ is derived in the last section as a function of antennas' and environment's characterstics. In this model, we have focused just on the physical characteristics of the receive side, and that is because to simplify the presentation of the principal concepts. Extending the analysis to the general case is straightforward and is based on the same roots developed here.

III. Role of Directional Antennas

By employing directional antennas one can improve the capacity expression in (4). An interesting problem is: what is the optimum antenna pattern which maximizes (4) among all possible patterns subject to $\int G(\theta)d\theta = 1$ (equal radiation power) ?

Considering this constraint, it is clear that the optimum pattern is:

$$G_{opt}(\theta) = \delta(\theta - \theta_{max}) \quad (5)$$

where $\delta(.)$ represents the delta function and

$$\theta_{max} = \arg\max(f_\Theta(\theta)) \quad (6)$$

This means that the optimal antenna maximizing the capacity is a highly directive antenna steered towards the most probable AoA (i.e., θ_{max}). By employing the optimal antenna, the capacity of the MIMO channel is as follows:

$$C_{max} = (2\pi n_r\gamma_0\log_2 e)f_\Theta(\theta_{max}) \quad (7)$$

It is clear that C_{max} is an upper bound for the capacity, since the directivity of practical antennas is bounded. In the case of using practical antennas, it is apparent that the main antenna beam should be steered towards θ_{max} as well. The capacity in this case is:

$$C = (2\pi n_r\gamma_0\log_2 e)\int_{-\pi}^{\pi} G(\theta)f_\Theta(\theta)d\theta \quad (8)$$

The following theorem proposes an approximate closed-form result for the capacity stated in (8) when using highly directive antennas.

Theorem 1: *In a MIMO system with n_t transmit antennas and n_r receive antennas, when employing highly directive antennas at the receiver to exploit the non-isotropic scattering environment around the receiver, the approximate capacity of system is expressed by:*

$$C \approx (4\pi n_r\gamma_0\log_2 e)\frac{\alpha_g}{2(1-e^{-\alpha_g\pi})}\mathcal{F}(\alpha_g) \quad (9)$$

where γ_0 is the transmitted SNR, $\mathcal{F}(s) = \mathcal{L}\{f_\Theta(\theta)\}$ represents the Laplace transform of the p.d.f. of AoA, and α_g satisfies the following equation:

$$\alpha_g = \arg\min_{\alpha}\left(\int_{-\pi}^{\pi}\left(G(\theta) - \frac{\alpha e^{-\alpha|\theta|}}{2(1-e^{-\alpha\pi})}\right)^2 d\theta\right) \quad (10)$$

which is the Minimum Mean Square Error (MMSE) criterion. Here, $G(\theta)$ and $f_\Theta(\theta)$ are antenna radiation pattern and p.d.f. of AoA respectively, with their maximum located at $\theta = 0$ and assumed to be even functions centered at $\theta = 0$. The approximation error is upper bounded by the following relation:

$$\begin{aligned} \mathcal{E} &= \frac{|C - C_{app}|}{(n_r\gamma_0\log_2 e)} \leqslant 4\pi\beta_1\sqrt{\int_0^{\pi} f_\Theta(\theta)^2 d\theta} \\ &+ (2D_0 + 4\pi\beta_2)e^{-(D_0 - 2\pi\beta_2)} \\ &\times \left(\int_0^{\infty} f_\Theta(\theta)d\theta - \frac{1}{2}\right) \end{aligned} \quad (11)$$

where the error bound depends on the antenna directivity, $D_0 = \max(2\pi G(\theta))$, and the error of approximating the antenna pattern with a Laplace function which is indicated in two error terms $\beta_1 = (\int_0^{\pi}(G(\theta) - \frac{\alpha_g e^{-\alpha_g\theta}}{2(1-e^{-\alpha_g\pi})})^2 d\theta)^{1/2}$, $\beta_2 = \max|G(\theta) - \frac{\alpha_g e^{-\alpha_g\theta}}{2(1-e^{-\alpha_g\pi})}|$.

Proof: First, we approximate $G(\theta)$ with the Laplace distribution with the parameter α_g:

$$G(\theta) \approx G^*(\theta, \alpha_g) = \frac{\alpha_g e^{-\alpha_g|\theta|}}{2(1-e^{-\alpha_g\pi})} \quad (12)$$

such that α_g satisfies (10). From (3) and (12) we derive:

$$E[|h|^2] = 4\pi \int_0^{\pi} \frac{\alpha_g e^{-\alpha_g \theta}}{2(1-e^{-\alpha_g \pi})} f_\Theta(\theta) d\theta \approx 4\pi \frac{\alpha_g}{2(1-e^{-\alpha_g \pi})} \mathcal{F}(\alpha_g) \quad (13)$$

where we have used the assumption of $G(\theta)$ being an even function which is a reasonable assumption in practical antennas because of their physical symmetry. Consequently, (9) is derived by using (13) and (4).

The approximation error can be written as the expression in (14) (top of the next page).

Thus, we will have:

$$\delta_1 = |4\pi \int_0^{\pi} f_\Theta(\theta)(G(\theta) - \frac{\alpha_g e^{-\alpha_g \theta}}{2(1-e^{-\alpha_g \pi})}) d\theta| \leqslant 4\pi \beta_1 \sqrt{\int_0^{\pi} f_\Theta(\theta)^2 d\theta} \quad (15)$$

where we have defined $\beta_1 = \{\int_0^{\pi} (G(\theta) - \frac{\alpha_g e^{-\alpha_g \theta}}{2(1-e^{-\alpha_g \pi})})^2 d\theta\}^{1/2}$, and have employed the Cauchy Schwartz inequality [11].

Also, we have

$$\delta_2 \leqslant 4\pi \frac{\alpha_g e^{-\alpha_g \pi}}{2(1-e^{-\alpha_g \pi})} (\int_0^{\infty} f_\Theta(\theta) d\theta - \frac{1}{2}) \quad (16)$$

We define $\beta_2 = \max_\theta |G(\theta) - \frac{\alpha_g e^{-\alpha_g \theta}}{2(1-e^{-\alpha_g \pi})}|$. Therefore, we will have: $|\frac{D_0}{2\pi} - \frac{\alpha_g}{2(1-e^{-\alpha_g \pi})}| \leqslant \beta_2$ and for the case of $\alpha_g \gg 1$ (highly directive antennas) we have: $|\frac{D_0}{2\pi} - \frac{\alpha_g}{2}| \leqslant \beta_2$, where D_0 is the antenna directivity. Consequently, we can find the following bound for δ_2:

$$\delta_2 \leqslant (2D_0 + 4\pi\beta_2) e^{-(D_0 - 2\pi\beta_2)} (\int_0^{\infty} f_\Theta(\theta) d\theta - \frac{1}{2}) \quad (17)$$

Finally, by using (14), (15) and (17) the bound stated in (11) is derived.

We observe that the error bound depends on the antenna directivity, D_0, and the error of approximating the antenna pattern with a Laplace function which is indicated in two error terms $\beta_1 = (\int_0^{\pi} (G(\theta) - \frac{\alpha e^{-\alpha \theta}}{2(1-e^{-\alpha \pi})})^2 d\theta)^{1/2}$, $\beta_2 = \max_\theta |G(\theta) - \frac{\alpha_g e^{-\alpha_g \theta}}{2(1-e^{-\alpha_g \pi})}|$. However, the right term is small compared to the left term in the case of highly directive antennas. Therefore, we conclude that a reasonable criterion for finding α_g is the MMSE criterion stated in (10). □

As mentioned above, a candidate for AoA p.d.f. in non-isotropic environments already proposed in the literature is the truncated Laplace distribution [10]. This p.d.f. is denoted as follows:

$$f_\Theta(\theta) = \frac{\alpha_s e^{-\alpha_s |\theta|}}{2(1-e^{-\alpha_s \pi})} \quad (18)$$

where α_s is a measure of how much non-isotopical the environment is. By employing Theorem 1 to this case, we have the following capacity expression:

$$C \approx (n_r \gamma_0 \log_2 e)(\frac{\pi}{\alpha_g + \alpha_s}) \times (\frac{\alpha_g}{1-e^{-\alpha_g \pi}})(\frac{\alpha_s}{1-e^{-\alpha_s \pi}}) \quad (19)$$

where α_g satisfies (10).

From (19), it can be verified that $\lim_{\alpha_g \to \infty} C = (n_r \gamma_0 \log_2 e) \frac{\pi \alpha_s}{1-e^{-\pi \alpha_s}} = (2\pi n_r \gamma_0 \log_2 e) \max(f_\Theta(\theta))$ as expected from our previous discussion of optimal antenna capacity.

For the non-isotropic scattering environment characterized by truncated Normal distribution [10] denoted by the following p.d.f.:

$$f_\Theta(\theta) = \alpha_s \frac{e^{-\frac{\alpha_s^2 \theta^2}{2}}}{\mathrm{erf}(\frac{\alpha_s \pi}{\sqrt{2}}) \sqrt{2\pi}} \quad (20)$$

and by applying Theorem 1, the capacity will be :

$$C \approx (\pi n_r \gamma_0 \log_2 e)(\frac{\alpha_g e^{\frac{\alpha_g^2}{2\alpha_s^2}}}{1-e^{-\alpha_g \pi}})(\frac{\mathrm{erfc}(\frac{\alpha_g}{\sqrt{2}\alpha_s})}{\mathrm{erf}(\frac{\pi \alpha_s}{\sqrt{2}})}) \quad (21)$$

where $\mathrm{erf}(.)$ and $\mathrm{erfc}(.)$ represent error function and complimentary error function respectively. By using the following asymptotic approximation, for large values of x, for the complimentary error function [12]:

$$\mathrm{erfc(x)} \approx \frac{\mathrm{e}^{-\mathrm{x}^2}}{\mathrm{x}\sqrt{\pi}} \sum_{\mathrm{n}=0}^{\infty} (-1)^{\mathrm{n}} \frac{(2\mathrm{n})!}{\mathrm{n}!(2\mathrm{x})^{2\mathrm{n}}} \quad (22)$$

It can be easily shown that $\lim_{\alpha_g \to \infty} C = 2\pi n_r \gamma_0 \log_2 e \max(f_\Theta(\theta))$ as expected from our previous discussion of optimal antenna capacity.

IV. Simulation Results for Capacity of Practical Directional Antennas

A. Square Microstrip Patch Antenna

The structure of a square microstrip patch antenna is depicted in Figure 1 (Figure adapted from [4]). The dimensions of the antenna are put the same (i.e., $L = W = \gamma \lambda_d = \gamma \lambda / \sqrt{\epsilon_r}$), where ϵ_r is the substrate dielectric constant put equal to 2.35. The radiation pattern considering the coordinates depicted in Figure 1 is [4]:

$$F(\theta, \phi) = \sqrt{\cos^2(\phi) + \sin^2(\phi)\cos^2(\theta)} f_1(\theta, \phi) \quad (23)$$

where

$$f_1(\theta, \phi) = \frac{\sin((\gamma\pi/\sqrt{\epsilon_r}) \sin(\theta) \sin(\phi))}{(\gamma\pi/\sqrt{\epsilon_r}) \sin(\theta) \sin(\phi)} \times \cos((\gamma\pi/\sqrt{\epsilon_r}) \sin(\theta) \sin(\phi)) \quad (24)$$

By putting $\phi = 90^o$ we will have:

$$F(\theta) = \cos(\theta) \frac{\sin((\gamma\pi/\sqrt{\epsilon_r}) \sin(\theta))}{(\gamma\pi/\sqrt{\epsilon_r}) \sin(\theta)} \cos((\gamma\pi/\sqrt{\epsilon_r}) \sin(\theta)) \quad (25)$$

The pattern is non-zero only in the upper hemisphere. Figure 2 depicts the radiation pattern of this antenna when $L = W =$

$$\begin{aligned}\frac{|C-C_{app}|}{n_r\gamma_0\log_2 e} &= |4\pi\int_0^{\pi} G(\theta)f_\Theta(\theta)d\theta - 4\pi\frac{\alpha_g}{2(1-e^{-\alpha_g\pi})}\mathcal{F}(\alpha_g)| \\ &\leqslant |4\pi\int_0^{\pi} G(\theta)f_\Theta(\theta)d\theta - 4\pi\frac{\alpha_g}{2(1-e^{-\alpha_g\pi})}\int_0^{\pi} e^{-\alpha_g\theta}f_\Theta(\theta)d\theta| + |4\pi\frac{\alpha_g}{2(1-e^{-\alpha_g\pi})}\int_{\pi}^{\infty} e^{-\alpha_g\theta}f_\Theta(\theta)d\theta| \\ &= \delta_1+\delta_2 \end{aligned} \quad (14)$$

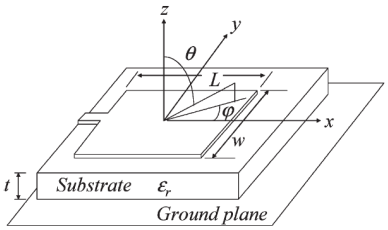

Fig. 1. Square Microstrip Patch Antenna Structure (Figure Adapted From [4])

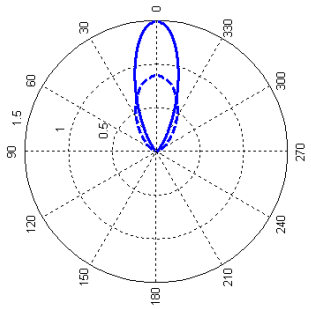

Fig. 2. Square Microstrip Patch Antenna Radiation Pattern vs. θ. Solid line is for $W = L = \lambda_d$ and dashed line is for $W = L = 0.5\lambda_d$.

$0.5\lambda_d$ and $L = W = \lambda_d$. Finally, $G(\theta)$ is the normalized power pattern (i.e., $G(\theta) = F(\theta)^2/\int F(\theta)^2 d\theta$).

Figure 3 depicts the capacity improvement of the system equipped with square microstrip patch antenna plotted versus α_s compared to the omnidirectional antenna case. The exact capacity and the proposed closed-form approximation results are plotted, where the non-isotropic scattering environment is characterized by the Laplace distribution with the parameter α_s. Two different antenna dimensions (i.e., $L = W = 0.5\lambda_d$ and $L = W = \lambda_d$) are considered in this figure. Figure 4 scenario is the same as that of Figure 3, but for the Normal distribution for the p.d.f. of AoA with the parameter α_s.

B. Horn Antenna

The horn antenna is also another example of a directional antenna. E-plane horn antenna pattern is depicted in Figure 5 (Figure adapted from [13]). In [13], by a novel approach, an E-plane radiation pattern approximation is proposed which is as follows:

$$F(\theta) = \frac{1}{2}[\frac{\sin(Kb\sin(\theta_0/2-\theta))}{Kb\sin(\theta_0/2-\theta)} +$$

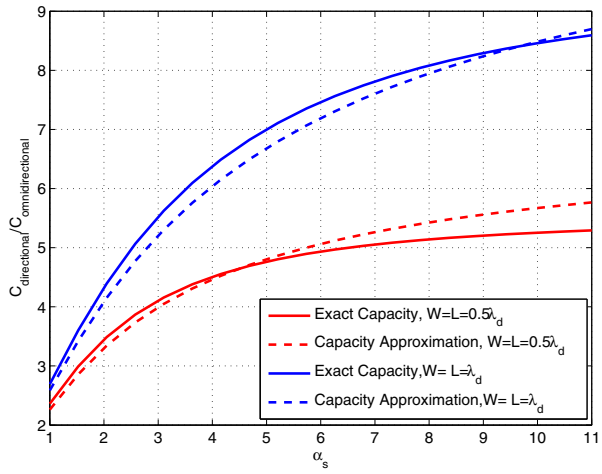

Fig. 3. Capacity enhancement due to using Square Microstrip Patch Antenna in non-uniform scattering environment characterized by Laplace p.d.f. for two cases: $W = L = 0.5\lambda_d$ and $W = L = \lambda_d$

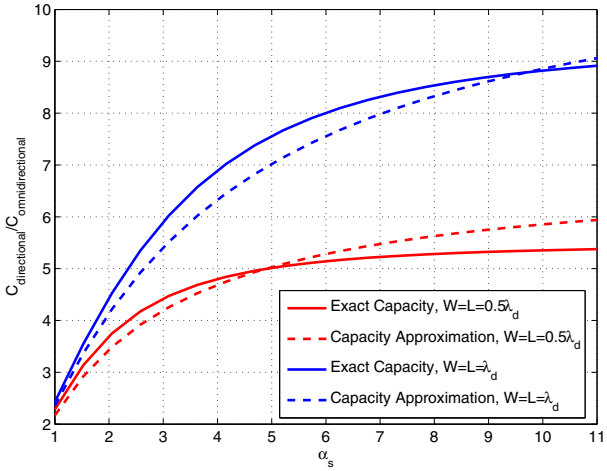

Fig. 4. Capacity enhancement due to using Square Microstrip Patch Antenna in non-uniform scattering environment characterized by Normal p.d.f. for two cases: $W = L = 0.5\lambda_d$ and $W = L = \lambda_d$

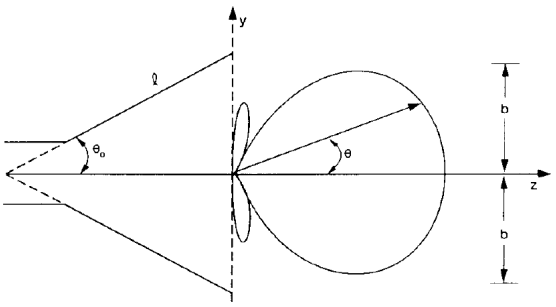

Fig. 5. E-plane horn antenna pattern. The opening angle of the horn is denoted by θ_0. (Figure adapted from [13].)

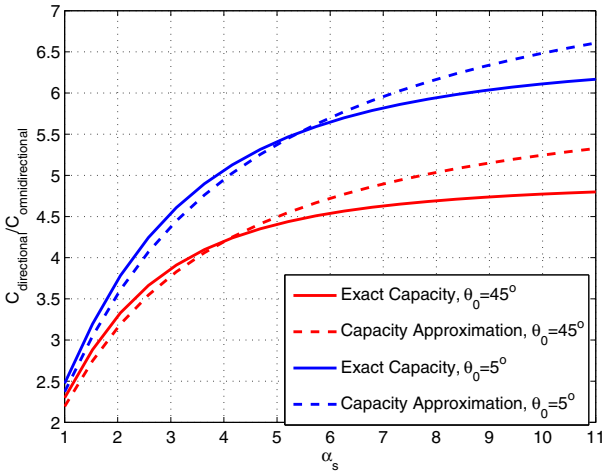

Fig. 6. Capacity enhancement due to using Horn Antenna in non-uniform scattering environment characterized by Laplace p.d.f. for two cases: $\theta_0 = 45^o$ and $\theta_0 = 5^o$

$$\frac{\sin(Kb\sin(\theta_0/2+\theta))}{Kb\sin(\theta_0/2+\theta)}] \qquad (26)$$

where $K = 2\pi/\lambda$ and λ is the wavelength. Figure 6 depicts the capacity improvement of the system equipped with horn antenna plotted versus α_s. The exact capacity and the proposed closed-form approximation results are plotted, where the non-isotropic scattering environment is characterized by the Laplace distribution with the parameter α_s. Two different opening angles for the horn antenna (i.e., $\theta_0 = 45^o$ and $\theta_0 = 5^o$) are considered in this figure. Figure 7 scenario is the same as that of Figure 6 but for the Normal distribution for the p.d.f. of AoA with the parameter α_s.

As it is clear in these figures, the capacity improvement depends on both the antenna directivity and the non-isotropic nature of the environment. These figures verify that the closed-form approximate results are matched very well with the exact results.

V. Conclusion

In this paper, we proposed an analytical approach to show the improvement of MIMO systems employing directional

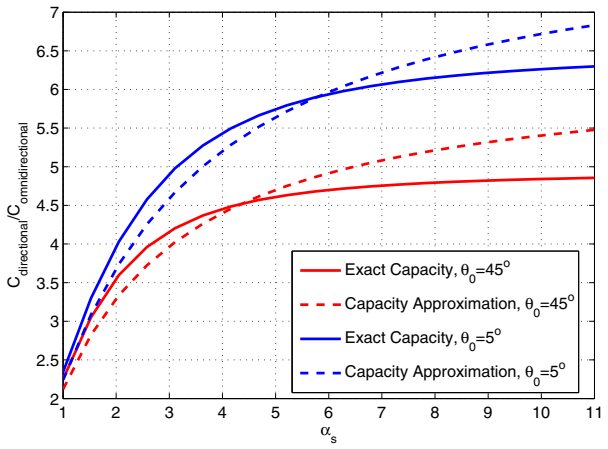

Fig. 7. Capacity enhancement due to using Horn Antenna in non-uniform scattering environment characterized by Normal p.d.f. for two cases: $\theta_0 = 45^o$ and $\theta_0 = 5^o$

antennas in non-isotropic scattering environments. Our analysis (performed in low-SNR regime) suggests that by proper steering of the MEAs' patterns, one can considerably improve the performance of a MIMO system in non-isotropic propagation environments. We have shown this fact by deriving closed-form approximate capacity expressions which agree very well with the exact values. In addition, we have shown that the capacity depends both on the environments physical characteristics as well as the antennas spatial directivity. Considering the fact that the analysis is valid for low-SNR regime, extension of results to other SNR regimes is of great importance.

VI. Acknowledgement

This work is supported by Iran Telecommunication Research Center (ITRC).

References

[1] G. J. Foschini and M. J. Gans, "On limits of wireless communications in a fading environment when using multiple antennas," Wireless Personal Communications, vol. 6, no. 3, pp. 311-335, 1998.

[2] P. Kyritsi, D. C. Cox, R. A. Valenzuela, and P. W. Wolniansky, *"Effect of Antenna Polarization on the Capacity of a Multiple Element System in an Indoor Environment,"* IEEE Journal on Selected Areas in Communications, Vol. 20, No. 6, August 2002.

[3] K. Sulonen, P. Suvikunnas, L. Vuokko, J. Kivinen, and P. Vainikainen, "Comparison of MIMO Antenna Configurations in Picocell and Microcell Environments," IEEE Journal on Selected Areas in Communications, Vol. 21, No. 5, June 2003.

[4] J. Gong, J. F. Hayes, M. R. Soleymani, *"The Effect of Antenna Physics on Fading Correlation and the Capacity of Multielement Antenna Systems,"* IEEE Tansactions on Vehicular Technology, Vol. 56, No. 4, July 2007.

[5] N. Razavi-Ghods, M. Abdalla and S. Salous, *"Characterisation of MIMO Propagation Channels Using Directional Antenna Arrays,"* IEE International Conference on 3G Mobile Communication Technologies (3G2004), London, October 2004.

[6] Shirook M. Ali, Wen Geyi, Qinjiang Rao, and Mark Pecen, *"Numerical Calculations of the Information Capacity of a Transmitting Antenna,"* white paper, Mobile Broadband Americas.

[7] D. Tse and P. Viswanath, *"Fundamentals of Wireless Communication,"* Cambridge University Press, 2005.

[8] A. Goldsmith, *"Wireless Communications,"* Cambridge University Press, 2005.
[9] C. A. Balanis, *"Antenna Theory, Analysis and Design,"* Harper & Row Publishers, 1982.
[10] H. Saligheh Rad and S. Gazor, *"The Impact of Non-Isotropic Scattering and Non-Omnidirectional Antennas on MIMO Communication Channels",* scheduled for publication in the IEEE Transactions on Communications, Volume 56, Issue 4, pp. 642 - 652, April 2008.
[11] D. G. Dudley, *"Mathematical Foundations for Electromagnetic Theory,"* Mir Publishers.
[12] M. Abramowitz and I. A. Stegun, eds. *Handbook of Mathematical Functions with Formulas, Graphs, and Mathematical Tables.* New York: Dover, 1972.
[13] P.D. Ewing, *"Approximation technique for determining gain and radiation pattern of the horn antenna,"* Southeastcon '89 Conference and Exhibition, Columbia, SC, 9 Apr. 1989.